Derivation of a New Smoke Emissions Inventory using Remote Sensing, and Its Implications for Near Real-Time Air Quality Applications

Luke Ellison
Science Systems and Applications, Inc., 10210 Greenbelt Road, Ste. 600, Lanham, MD, 20706
NASA Goddard Space Flight Center, Code 613, Greenbelt, MD 20771
luke.ellison@nasa.gov

Charles Ichoku
NASA Goddard Space Flight Center, Code 613, Greenbelt, MD 20771
charles.ichoku@nasa.gov

ABSTRACT

A new emissions inventory of particulate matter (PM) is being derived mainly from remote sensing data using fire radiative power (FRP) and aerosol optical depth (AOD) retrievals from the Moderate Resolution Imaging Spectroradiometer (MODIS) instrument, as well as wind data from the Modern Era Retrospective-Analysis for Research and Applications (MERRA) reanalysis dataset, which spans the satellite era. This product is generated using a coefficient of emission, C_e, that has been produced on a 1×1° global grid such that, when it is multiplied with satellite measurements of FRP or its time-integrated equivalent fire radiative energy (FRE) retrieved over a given area and time period, the corresponding PM emissions are estimated. This methodology of using C_e to derive PM emissions is relatively new and advantageous for near real-time air quality applications compared to current methods based on post-fire burned area that may not provide emissions in a timely manner. Furthermore, by using FRP to characterize a fire's output, it will represent better accuracy than the use of raw fire pixel counts, since fires in individual pixels can differ in size and strength by orders of magnitude, resulting in similar differences in emission rates. Here we will show examples of this effect and how this new emission inventory can properly account for the differing emission rates from fires of varying strengths. We also describe the characteristics of the new emissions inventory, and propose the process chain of incorporating it into models for air quality applications.

INTRODUCTION

Fires are a global phenomenon that persists in six of the seven continents (except in ice-covered Antarctica), and can affect not only the local climate, but also the global climate as a whole. Wildfires emit vast amounts of smoke comprising particulate matter (PM), trace gases and water vapor into the atmosphere. Unlike most other phenomena that affect climate variability, such as sea surface temperature that changes relatively slowly, the sporadic occurrence and rapidly evolving nature of fires makes them particularly difficult to characterize and monitor. However, to understand the impact of fires on air quality and climate systems, and therefore on human health and climate change, smoke emission is a critical process that needs to be well understood at local, regional and global scales.

Characterizing the smoke emission output from fires at regional to global scales is being enabled by satellite observations, unlike the pre-satellite era when such activities were only local in scope. Within the last decade, the number of satellite-based smoke emissions inventories has been increasing as scientists are researching different methods for deriving accurate PM emissions from direct observation of active fires. One of the first such methods proposed was that of *Ichoku & Kaufman* (2005)[1] that uses fire and aerosol observational data from satellite to generate a coefficient of emission, C_e, that relates fire strength to its PM emissions. Work on this algorithm has continued and is currently resulting in a first version of an emissions product by the Fire Energetics and Emissions Research (FEER)[2] project group. This paper summarizes the algorithm used to generate coefficients of emission and subsequently

describes the process chain that shows how this data can be used to generate emissions from satellite measurements of fire radiative energy (FRE) release rate or power (FRP), which can then be input into models for forecasting or monitoring purposes.

METHODOLOGY

Smoke Emissions from Satellite Observations

Several methods have been proposed for estimating emissions on a global scale. The traditional method used to estimate different species of particulate or gaseous emissions is described in e.g. *Andreae and Merlet* (2001)[3] as,

Equation (1) $M_x = EF_x \cdot M_{biomass}$

where

M_x = mass of emitted smoke species x
EF_x = emission factor of emitted smoke species x
$M_{biomass}$ = dry mass of combusted fuel

$M_{biomass}$ is often calculated from *Seiler and Crutzen* (1980)[4] as,

Equation (2) $M_{biomass} = A \cdot B \cdot \alpha \cdot \beta$

where

A = burned area
B = biomass density
α = fraction of above ground biomass
β = burn efficiency

However, the variables used in Equation 2 are difficult or even impossible to measure accurately and on a large and global scale. With the advent of fire detection algorithms from satellite, notably on the Moderate Resolution Imaging Spectroradiometer (MODIS) that flies on both the Earth Observing System (EOS) Terra and Aqua platforms, new methods have been able to estimate some of these parameters via conversion from fire pixel counts and other vegetation or fire-related satellite observations. One such emissions inventory that has been widely used for analyzing global emissions from wildfire is the Global Fire Emissions Database (GFED).[5,6]

It has been recognized, however, that fire pixel counts represent only a qualitative measurement of fire activity since fire intensities can vary by several orders of magnitude and also, in the case of MODIS for instance, a pixel ground footprint area can also vary by an order of magnitude, thereby adding more uncertainty in extending quantitative analyses to fire pixel count data.[7] Consequently, new smoke emission inventories currently being produced have been shifting towards the use of fire radiative power (FRP) and its temporally integrated fire radiative energy (FRE), which are quantitative measurements of emitted radiant energy of fires. Some such examples of FRP-based or related emissions inventories are the QFED[8], GFAS[9] and FLAMBE[10] products.

The Fire Energetics and Emissions Research (FEER, http://feer.gsfc.nasa.gov/)[2] project group is currently producing a new smoke emissions product in accordance with the method outlined in *Ichoku and Kaufman* (2005),[1] with some necessary updates to the algorithm. However, this product is unique in the sense that it is based solely on empirical methods using observational measurements of both FRP and AOD from MODIS to determine the rates of emission for a given region. The algorithm methodology is outlined in the next section.

Coefficient of Emission Gridded Product

The premise of the *Ichoku and Kaufman* (2005)[1] paper is that fire radiative energy (FRE), or the temporal integral of fire radiative power (FRP), is directly proportional to the amount of dry biomass combusted[11] and that the release of specific aerosols or trace gases is also directly proportional to the dry mass combusted according to Equation 1. It then logically follows that the mass of smoke aerosol, for instance, can be linearly related to FRE, without the complexity of determining A, B, α, β or even EF_{PM}. Similarly, the rate of aerosol emission can be related to that of FRE release (i.e. FRP). Thus, the following relationships are established:

Equation (3) $R_{sa} = C_e \cdot FRP$
Equation (4) $M_{sa} = C_e \cdot FRE$

where

R_{sa} = rate of smoke aerosol emission
M_{sa} = mass of smoke aerosol emission
C_e = coefficient of emission

The coefficient of emission, or C_e, is the coefficient that directly relates radiative power from a fire to its smoke aerosol emission rate. This study currently only focuses on generating C_e for PM emissions, although work is being done to extend this product to other common emitted species. For a given species such as PM, different C_e values are expected for different biome types and locations. Thus, a C_e product has been generated on a 1×1° global grid such that FRE measurements within any of the grid cells multiplied by the corresponding C_e values according to Equation 4 should consistently give the PM emissions generated from those fires.

In order to generate this C_e product, it was noted from Equation 3 that C_e can be taken as the slope of the trend line of the scatterplot between R_{sa} and FRP for each grid cell. FRP is easily obtained from the MODIS fire product (MOD14/MYD14);[12,13] R_{sa} can be estimated from the difference between background AOD measurements and those affected by the smoke plume using the MODIS aerosol product (MOD04_L2/MYD04_L2),[14,15] and from wind vectors from the Modern Era Retrospective-Analysis for Research and Applications (MERRA) reanalysis[16,17] or similar dataset. The original algorithm as described in *Ichoku and Kaufman* (2005)[1] calculates R_{sa} initially on a per-pixel basis as the total smoke aerosol mass, M_{sa}, over the time, T, it takes the smoke to clear the designated area. T is estimated using pixel geometry and 850 mbar (corresponding to an altitude of about 1.5 km) wind speed data from the meteorological datasets. M_{sa} is calculated as the product of the pixel area and the aerosol mass density, M_d, which in turn is estimated from the surrounding AOD values at 550 nm. The updated and current algorithm expands on its predecessor by using wind direction as well to more accurately determine AOD associated with the plume, and to determine if there is an influx of smoke generated elsewhere into the vicinity of the fire under consideration. Wind magnitudes are also used in conjunction with relative fire locations within an aerosol pixel to improve values of T. R_{sa} and preceding parameters are also calculated first on a per-pixel basis before aggregating the calculations to a regional or grid-basis, thereby theoretically reducing the uncertainty in estimating these parameters on a larger scale.

Once the pixel-level smoke emission rates were generated using data from both Terra and Aqua for the years 2003-2010, the values for R_{sa} and FRP were aggregated into 1×1° grid cells for the entire globe. However, as part of this process of aggregation and in order to remove contaminated data, certain key parameters and corresponding thresholds were identified and filtered out of the dataset. Thus, the resulting filtered dataset produced much cleaner results, showing clear trends that were previously undetectable. There were still a few examples, however, where clear outliers were adversely affecting

the trend line of the scatterplots between R_{sa} and FRP measurements, and so an outlier correction algorithm was also created specifically for use with the type of non-normal distribution of points observed between R_{sa} and FRP. This outlier algorithm was able to correct several misleading results, after which the final aggregation of the data within each grid cell was performed. The resulting C_e gridded map is shown in Figure 1. Individual C_e maps were generated for both Terra and Aqua data, but having observed that the differences between the two are not biased in any one direction, the two datasets were combined to gain greater spatial coverage. Figure 1 currently only shows values with the highest level of confidence.

Figure 1. Coefficients of emission are plotted globally on a 1×1° map. These values were obtained using an updated algorithm to that described in *Ichoku and Kaufman* (2005),[1] by fitting trends between FRP and R_{sa} generated from MODIS FRP and AOD data from both Terra and Aqua from 2003-2010.

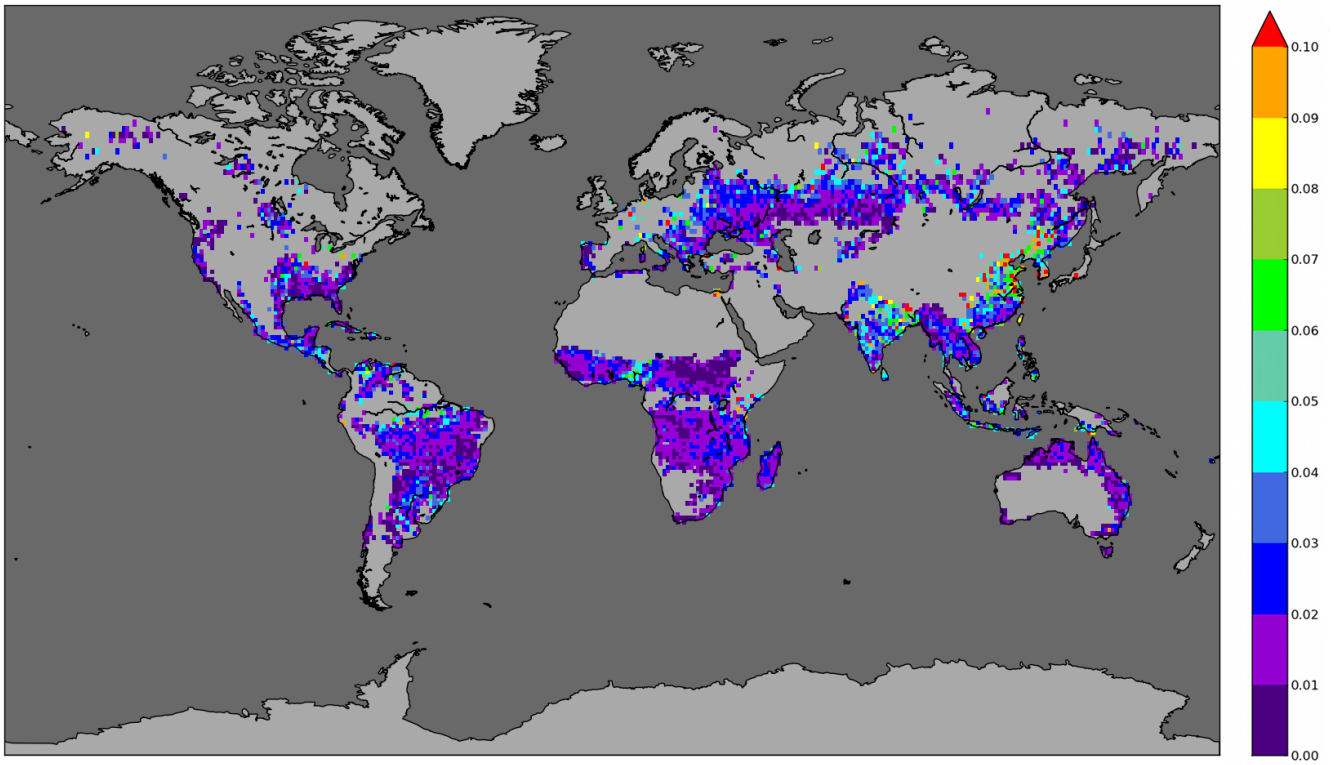

RESULTS AND CONCLUSIONS

Using C_e to Generate PM Emissions

In much the same way as C_e was generated using Equation 3 (as viewed in Figure 1), the C_e values can be used along with any given FRP measurements from any instrument for a particular region to determine the instantaneous emission rate using Equation 3 or its emissions over a certain time period using Equation 4. An example of this process is given in Figure 2 using FRP data observed by the SEVIRI sensor aboard the Meteosat geostationary satellite, as calculated by the Land Surface Analysis Satellite Applications Facility (LSA SAF)[18] for northern sub-Saharan Africa. One measurement of the hourly FRP product at 13:00 GMT on January 1, 2010 was extracted and appropriately multiplied against the C_e product to produce emission rates across the region for that time of observation. Notice how C_e modulates the PM emission rate relative to how much radiative power is being produced in each grid cell.

Figure 2. The LSA SAF FRP dataset from SEVIRI outputs hourly FRP values on a 1×1° grid over Africa. FRP values over northern sub-Saharan Africa are shown from January 1, 2010 at 13:00 GMT in the left-hand image, whereas the right-hand image is the corresponding emission rates generated using FEER's emissions algorithm.

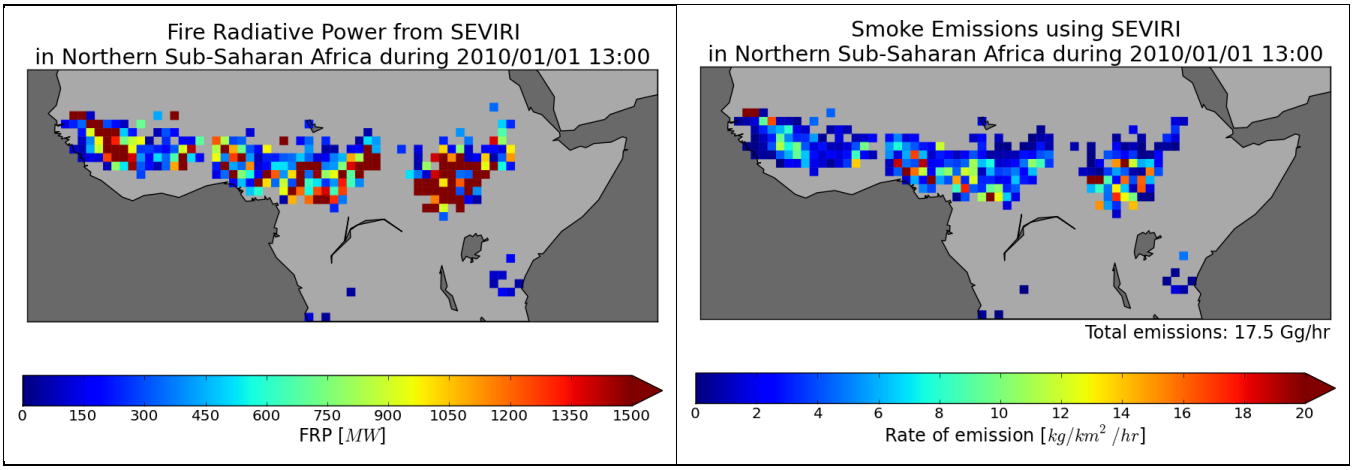

In order to obtain the total emissions for a given region and time period using Equation 4, however, the FRE corresponding to that region and time period needs to be accurately known. FRE is derived by integrating successive FRP measurements over a desired time period using a sufficiently small time step in order to be accurately resolved. Given that SEVIRI is able to measure FRP frequently over Africa, FRP data from the LSA SAF product has been integrated over January 2010 for northern sub-Saharan Africa, and then multiplied by C_e to produce the total PM emissions over the region for that time period (see Figure 3).

Figure 3. Hourly LSA SAF FRP values were temporally integrated over the month of January 2010 to generate the FRE values over northern sub-Saharan Africa as shown in the left-hand image. Total PM emissions corresponding to that time period that were generated using FEER's emissions algorithm is shown in the right-hand image.

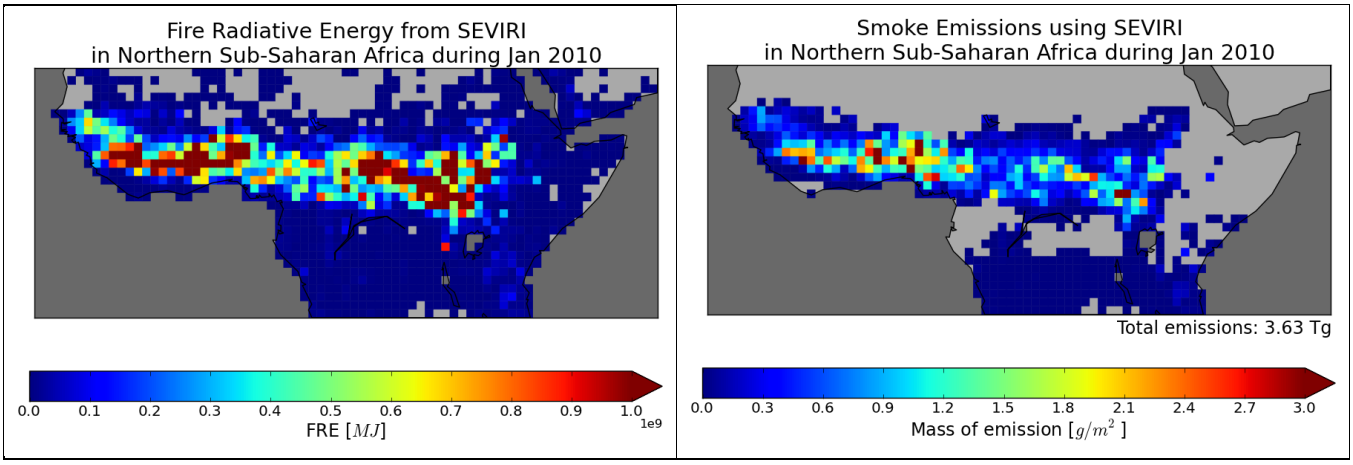

According to *Kaiser et al.* (2012),[9] GFASv1.0 reports an average annual emission of 7.874 Tg/yr and GFED3.1 reports 8.822 Tg/yr over the northern hemispherical Africa region ("NHAf"). In comparison, this FEER emissions algorithm reports about 12.2 Tg over the same region for the year 2010. This somewhat higher value is only based on one year's worth of data for one region and emission species, but the emission output in this region is fairly stable from year to year and therefore this result is certainly suggestive of the higher emissions that this algorithm is expected to generate, as is also indicated in the aforementioned paper.

Implications for Air Quality and Chemical Transport Modeling

Biomass burning contributes a substantial percentage of global PM emissions that can have a major impact on air quality and climate. It has been repeatedly reported by modelers that current databases significantly underestimate these PM emissions.[6,19] As such, it is crucial that an accurate database of PM emissions from fires be made available to modelers to improve results. The approach taken in this paper in an effort to reduce the current uncertainty is a top-down approach whereby observations of both fire and the emitted PM are made and directly correlated, bypassing the use of emission factors and other ancillary parameters that are difficult to determine (see Equation 2). As mentioned in the previous section, initial results show that for Northern Africa, an increase in PM emissions has been obtained using the *Ichoku and Kaufman* (2005)[1] updated algorithm described in this paper.

This top-down method of deriving PM emissions was originally developed based on the fact that *Ichoku and Kaufman* (2005)[1] found reasonable correlation between FRP and smoke PM emission rates for different biomes and regions, and by downscaling the process, a global gridded map of C_e has been derived. This product will provide modelers with a near real-time, flexible method of generating PM emissions. This capability is made possible by virtue of the fact that C_e is a relatively static product that will be updated only on an annual or multi-annual basis. Therefore, given the relative stability of this product a user may generate his/her own emissions databases simply by using different sources of FRP measurements from different sensors over different regions, without going through the entire retrieval process. The lag time in generating emissions from C_e is constrained only by that of obtaining FRP retrievals.

Finally, it should be noted that a global emissions product for fire-emitted PM using C_e is in the process of being created by the FEER project group, and will be made publically available upon completion. Furthermore, research is also being pursued to expand the product to include emissions of a number of other major aerosol and gaseous components of fire emissions for air quality and other modeling applications.

REFERENCES

1) Ichoku, C. and Y. J. Kaufman. "A method to derive smoke emission rates from MODIS fire radiative energy measurements", IEEE Trans. Geosci. Remote Sens. 2005, 43 (11), 2636–2649.
2) Ichoku, C. and L. Ellison. *Fire Energetics and Emissions Research*. NASA Goddard Space Flight Center, Greenbelt, MD, 2012. <http://feer.gsfc.nasa.gov>
3) Andreae, M. O. and P. Merlet. "Emission of trace gases and aerosols from biomass burning", Global Biogeochem. Cycles. 2001, 15, 955–995.
4) Seiler, W. and P. J. Crutzen. "Estimates of gross and net fluxes of carbon between the biosphere and the atmosphere from biomass burning", Clim. Change. 1980, 2, 207–248.
5) van der Werf, G. R., J. T. Randerson, L. Giglio, G. J. Collatz, P. S. Kasibhatla, and A. F. Arellano Jr. "Interannual variability in global biomass burning emissions from 1997 to 2004", Atmos. Chem. Phys. 2006, 6, 3423-3441.
6) van der Werf, G. R., J. T. Randerson, L. Giglio, G. J. Collatz, M. Mu, P. S. Kasibhatla, D. C. Morton, R. S. DeFries, Y. Jin, and T. T. van Leeuwen. "Global fire emissions and the contribution of deforestation, savanna, forest, agricultural, and peat fires (1997–2009)", Atmos. Chem. Phys. 2010, 10, 11707-11735.
7) Ichoku, C., L. Giglio, M. J. Wooster, L. A. Remer. "Global characterization of biomass-burning patterns using satellite measurements of fire radiative energy", Remote Sensing of Environment. 2008, 112 (6), 2950-2962.
8) van Donkelaar, A., R. V. Martin, R. C. Levy, A. M. da Silva, M. Krzyzanowski, N. E. Chubarova, E. Semutnikova, A. J. Cohen. "Satellite-based estimates of ground-level fine particulate matter during

extreme events: A case study of the Moscow fires in 2010", Atmospheric Environment. 2011, 45 (34), 6225-6232.

9) Kaiser, J. W., A. Heil, M. O. Andreae, A. Benedetti, N. Chubarova, L. Jones, J.-J. Morcrette, M. Razinger, M. G. Schultz, M. Suttie, and G. R. van der Werf. "Biomass burning emissions estimated with a global fire assimilation system based on observed fire radiative power", Biogeosciences. 2012, 9, 527-554.
10) Reid, J. S., E. J. Hyer, E. M. Prins, D. L. Westphal, J. Zhang, J. Wang, S. A. Christopher, C. A. Curtis, C. C. Schmidt, D. P. Eleuterio, K. A. Richardson, and J. P. Hoffman. "Global Monitoring and Forecasting of Biomass-Burning Smoke: Description of and Lessons From the Fire Locating and Modeling of Burning Emissions (FLAMBE) Program", IEEE Journal of Selected Topics in Applied Earth Observations and Remote Sensing. 2009, 2 (3), 144-162.
11) Wooster, M. J., G. Roberts, G. L. W. Perry, and Y. J. Kaufman. "Retrieval of biomass combustion rates and totals from fire radiative power observations: FRP derivation and calibration relationships between biomass consumption and fire radiative energy release", J. Geophys. Res. 2005, 110, D24311.
12) Giglio, L., Descloitres, J., Justice, C.O., Kaufman, Y. "An enhanced contextual fire detection algorithm for MODIS", Remote Sensing of Environment. 2003, 87, 273-282.
13) Justice, C., L. Giglio, L. Boschetti, D. Roy, I. Csiszar, J. Morisette, and Y. Kaufman. *MODIS Fire Products Algorithm Technical Background Document*. 2006, Version 2.3, EOS ID# 2741.
14) Remer, L. A., Y. J. Kaufman, D. Tanre, S. Mattoo, D. A. Chu, J. V. Martins, R. R. Li, C. Ichoku, R. C. Levy, R. G. Kleidman, T. F. Eck, E. Vermote, B. N. Holben. "The MODIS aerosol algorithm, products, and validation", J. Atmos. Sci. 2005, 62 (4), 947–973.
15) Levy, R. C., L. A. Remer, D. Tanre, S. Mattoo, Y. J. Kaufman. *Algorithm for Remote Sensing of Tropospheric Aerosol over Dark Targets from MODIS: Collections 005 and 051*. 2009, Revision 2, 96.
16) Acker J. G., and G. Leptoukh. "Online Analysis Enhances Use of NASA Earth Science Data", Eos, Trans. AGU. 2007, 88 (2), 14 and 17.
17) Rienecker, M. M., M. J. Suarez, R. Todling, J. Bacmeister, L. Takacs, H.-C. Liu, W. Gu, M. Sienkiewicz, R. D. Koster, R. Gelaro, I. Stajner, and J. E. Nielsen. *The GEOS-5 data assimilation system—Documentation of versions 5.0.1 and 5.1.0, and 5.2.0*, NASA Tech. Rep. Series on Global Modeling and Assimilation, NASA Goddard Space Flight Center, Greenbelt, MD, 2008; NASA/TM-2008-104606, 27.
18) Govaerts, Y. M., M. Wooster, A. Lattanzio, G. Roberts. *MSG/SEVIRI Fire Radiative Power (FRP) Characterisation ATBD*, EUMETSAT, 2007; Report EUM/MET/SPE/06/0398, pp 32.
19) van der Werf, G. R., J. T. Randerson, G. J. Collatz, L. Giglio, P. S. Kasibhatla, A. F. Arellano, Jr., S. C. Olsen, E. S. Kasischke. "Continental-Scale Partitioning of Fire Emissions During the 1997 to 2001 El Niño/La Niña Period", Science. 2004, 303 (5654), 73-76.

KEY WORDS

Emissions
Fire
Biomass Burning
Smoke
PM
Fire Radiative Power (FRP)
Fire Radiative Energy (FRE)
MODIS
Remote Sensing
Air Quality